JOURNAL OF MATERIALS SCIENCE 29 (1994) 2395–2400

Multiphase composites of tetragonal zirconia agglomerate dispersed into alumina and alumina–zirconia matrices

TADASHI ENDO, NAOMICHI MIYAGAWA, HIROTSUGU TAKIZAWA, MASAHIKO SHIMADA
Department of Molecular Chemistry and Engineering, Faculty of Engineering, Tohoku University, Aoba-ku, Sendai, Miyagi 980, Japan

Multiphase composites of yttria- and ceria-doped tetragonal zirconia agglomerates (10–50 μm) dispersed into an alumina or alumina–zirconia matrix were sintered at 1500–1600 °C in air, followed by post-Hot Isostatic Pressing (HIP) at 1450 °C and 150 MPa in an Ar gas atmosphere. The relative density of the recovered composites was above 98% of the theoretical density. By chemically etching on the surface of zirconia agglomerates, the sinterability of composites was apparently improved; and no microcracks nor pores were observed at the interface of agglomerate and matrix. According to scanning electron microscopy (SEM) observation, tetragonal and tetragonal–monoclinic zirconia agglomerates were highly dispersed into the alumina or alumina–zirconia matrix. The multiphase composites containing 10 vol% spherical agglomerates demonstrate the relatively low value of bending strength, < 400 MPa, and a high value of fracture toughness, > 11 MPa $m^{1/2}$. The crack propagation introduced by Vickers indentation was efficiently suppressed and deflected by the agglomerates.

1. Introduction

Alumina (Al_2O_3) is an attractive material for wear and structural application because of its superior physical properties, such as high melting point, elasticity, hardness and resistance to chemical corrosion. Recently, with the technological development of fine powder processing and sintering, a high fracture strength value of 500 MPa was reported for commercially available alumina ceramic [1]. However, the fracture toughness was not high enough to apply the monolithic alumina as a structural ceramic under a high stress field because of its fragility. Consequently, it is highly expected to increase further the fracture toughness of alumina ceramics.

Uniform dispersion of second phase fragments, such as whisker fibre particles, etc., into the fragile ceramic is more efficacious for improvement of the fracture toughness [2, 3]. The increase of fracture toughness is usually attributed to the interaction of the crack front with the second phase fragments, i.e. pinning or bowing of the crack front by the second phase fragments, microcrack formation in the crack-tip region, and stress-induced phase transformation.

It is well known that dispersion of tetragonal zirconia particles into the alumina matrix is a readily available technique for toughening alumina ceramics [4]. Very recently, Stevens and Evans [5] pointed out that the "duplex structure" could absorb the fracture energy or dissipate the microcrack, thereby increasing the toughness of the ceramics. The microstructure was composed of polycrystalline agglomerates of zirconia in a matrix of fine grained alumina.

Many experimental and theoretical studies on the fabrication of ceramic composites indicated that the densification of polycrystalline powders was substantially retarded by the presence of second phase fragments of large size, even at relatively low volume fractions. However, the densification behaviour of composites containing second phase fragments, especially those such as agglomerates, has not been satisfactorily understood [6]. In the present study, a series of fabrication experiments of multiphase composites was carried out, in which various amounts of ZrO_2 and yttria- and ceria-doped tetragonal zirconia polycrystalline agglomerates were uniformly dispersed into the alumina and alumina–zirconia matrices to improve fracture toughness.

2. Experimental procedure

Al_2O_3 powder, coprecipitated fine grain ZrO_2 powder containing 0 and 3 mol % Y_2O_3 (denoted as TZO and TZ-3Y) and 12 mol % CeO_2 (denoted as TZ-12Ce) were used as starting materials.

TZO, TZ-3Y and TZ-12Ce powders were calcined at 1500 °C for 10 h in air to form zirconia agglomerates with monoclinic phase for TZO, and tetragonal phase for TZ-3Y and TZ-12Ce. The resulting agglomerates were chemically etched in hot concentrated

0022–2461

H_2SO_4 solution for 24 h in order to activate chemically their surface, and were recovered by filtrating. The products were intimately mixed with Al_2O_3, TZO, TZ-3Y and TZ-12Ce powders by ball-milling using plastic containers and balls with a small amount of ethanol for 24 h. Successively, the mixtures were isostatically pressed at 200 MPa to form plates ($5 \times 30 \times 50$ mm) and sintered at 1600 °C for 10 h in air. The rates of heating and cooling were fixed throughout to about 1.5 °C min^{-1}. Occasionally, the presintered composites, except those containing TZ-12Ce particles, were hot isostatically pressed (HIP) at 1450 °C and 150 MPa for 1 h under an Ar gas atmosphere.

Phase identification of the recovered sample was carried out by means of X-ray powder diffraction with monochromatic CuK_α radiation. The bulk density of the sample was determined by the Archimedes technique. The microstructure of samples was observed under SEM. Fracture toughness of the samples was determined by an indentation fracture method at room temperature [7]. The fracture strength of the sample was measured by a three-point bending test with a crosshead speed of 0.5 mm min^{-1} and a span width of 10 mm [8].

3. Results and discussion

Figs 1, 2 and 3 show SEM photographs of polycrystalline agglomerates, TZO, TZ-3Y and TZ-12Ce,

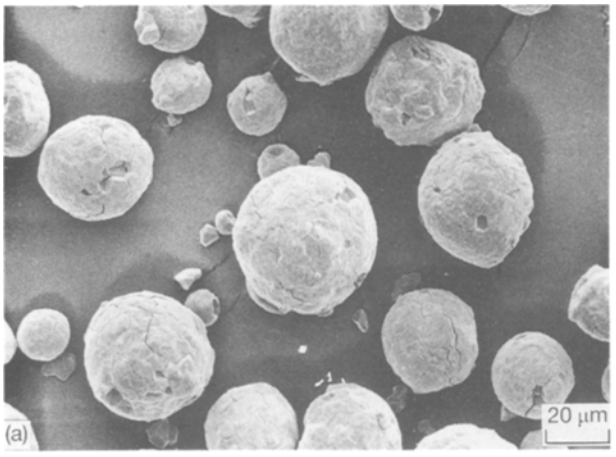

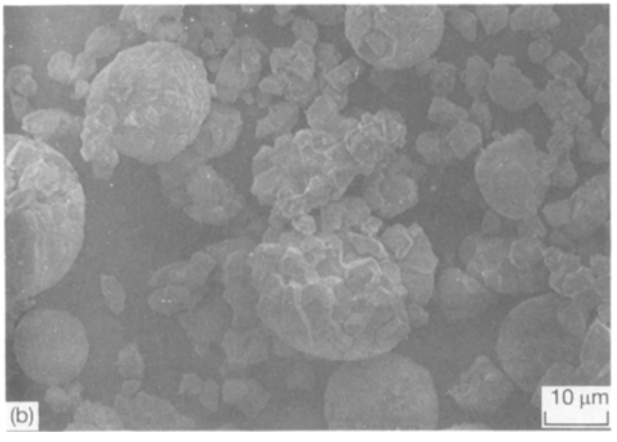

Figure 1 SEM photograph showing the calcined TZO agglomerates (a) before etching and (b) after etching.

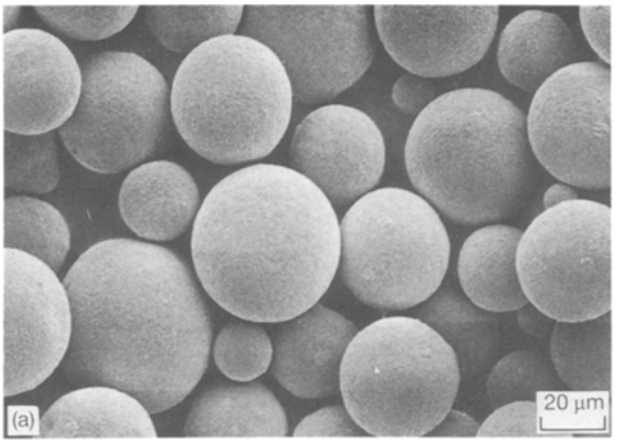

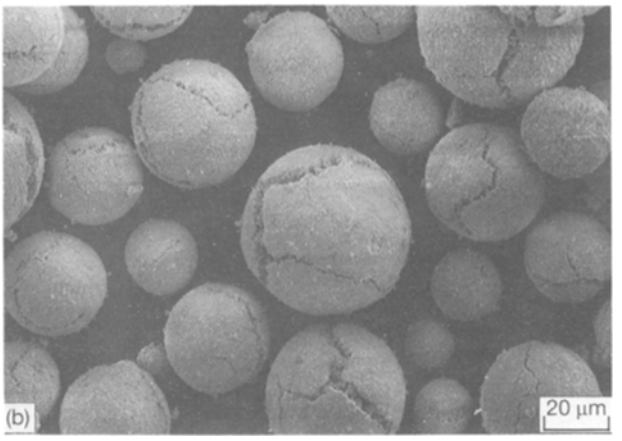

Figure 2 SEM photograph showing the calcined TZ-3Y agglomerates (a) before etching and (b) after etching.

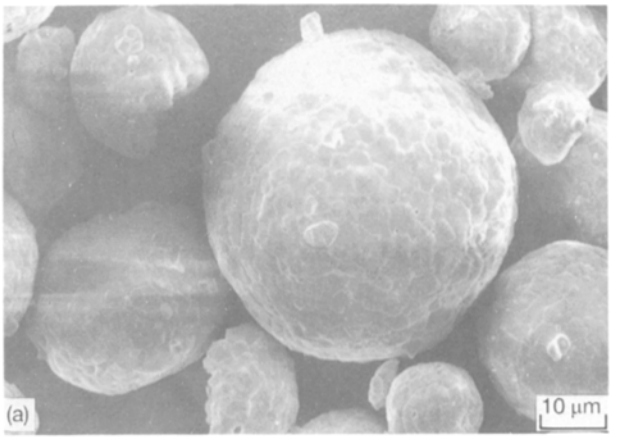

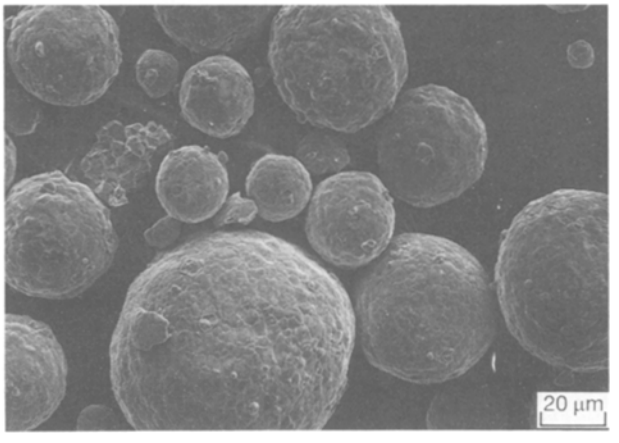

Figure 3 SEM photograph showing the calcined TZ-12Ce agglomerates (a) before etching and (b) after etching.

before and after chemical etching in the hot concentrated H_2SO_4 solution, respectively. It was found that the fine zirconia particles were spontaneously coagulated to form spherical agglomerates of about 50 μm in size. However, the etching profile was fairly different among agglomerates with various sintering agents. By etching, TZO agglomerates fell to pieces, and TZ-3Y agglomerates developed pomegranate-like structures fissured to their surfaces (Figs 1 and 2). From the results of X-ray powder diffraction analysis, it was confirmed that ZrO_2 changed partially from tetragonal to monoclinic form on the skin of TZ-3Y agglomerates. Accordingly, the observed macrocracks could be caused by the phase transformation, with 3–5% volume expansion of the agglomerate. On the other hand, chemical etching at the grain boundary of TZ-12Ce agglomerates was observed, and no phase transformation occurred. As a result, the solubility difference between yttrium and cerium ions, as stabilized cations for the tetragonal phase in the hot concentrated H_2SO_4 solution, was considerably reflected in the surface structure of the resulting composites.

Figs 4, 5 and 6 show polished cross-sections of composites, containing etched TZO, TZ-3Y and TZ-12Ce agglomerates, in Al_2O_3 matrices sintered at 1600 °C for 10 h in air, respectively. Most of the zirconia agglomerates (indicated by lightened parts in the SEM photographs) kept their initial shape and size. In the case of TZ-3Y–Al_2O_3 composite, some macrocracks intersected drastically in the alumina matrix. It was considered that the macrocracks within the alumina matrix were substantially brought about by swelling of the agglomerate during the t → m phase transformation. In the case of the TZ-12Ce–Al_2O_3 composite, uniformly dispersed agglomerates were observed in the alumina matrix without macrocracks. It was, therefore, found that the duplex structure was designed and fabricated by using the presintered and etched zirconia agglomerates.

Figs 7 and 8 are SEM photographs of the fracture surfaces of the composites containing TZ-12Ce agglomerates, with and without chemical etching, respectively. The surface activities of TZ-12Ce agglomerates are responsible for the transgranular and the intergranular fracture modes, i.e. the fracture is clearly experienced at the boundary between the cluster and the matrix for composites containing agglomerates without chemical etching, but occurs at interclusters for composites containing agglomerates with chemical etching.

The relative densities of composites with 20 vol % zirconia particles in the alumina matrix (sintered at

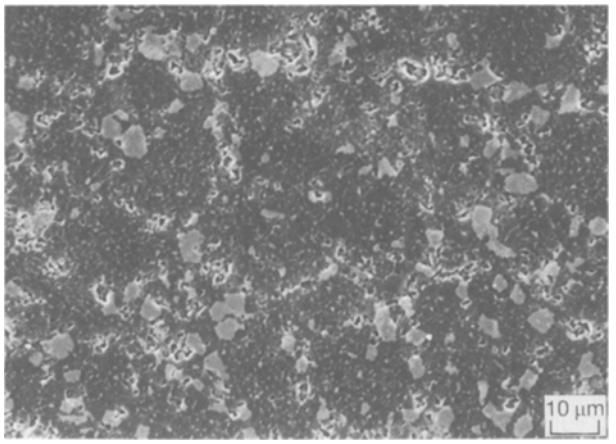

Figure 4 SEM photograph showing a polished cross-section of composites with 20 vol % TZO agglomerate.

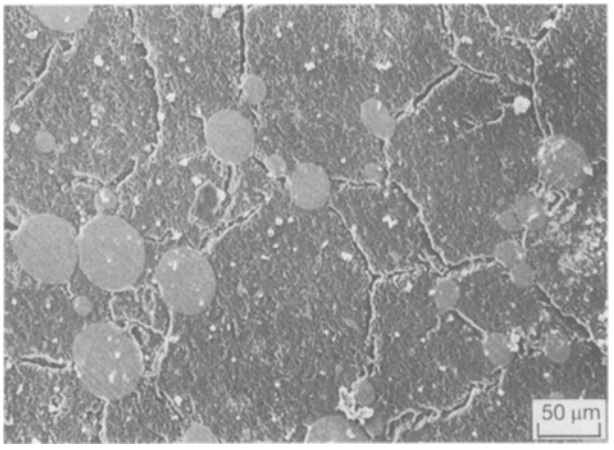

Figure 5 SEM photograph showing a polished cross-section of composites with 20 vol % TZ-3Y agglomerate.

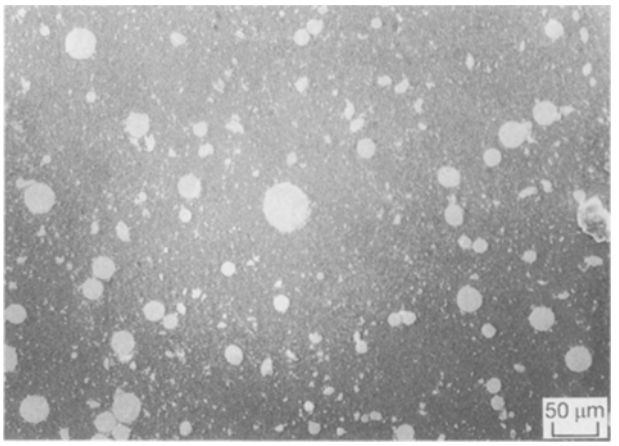

Figure 6 SEM photograph showing a polished cross-section of composites with 20 vol % TZ-12Ce agglomerate.

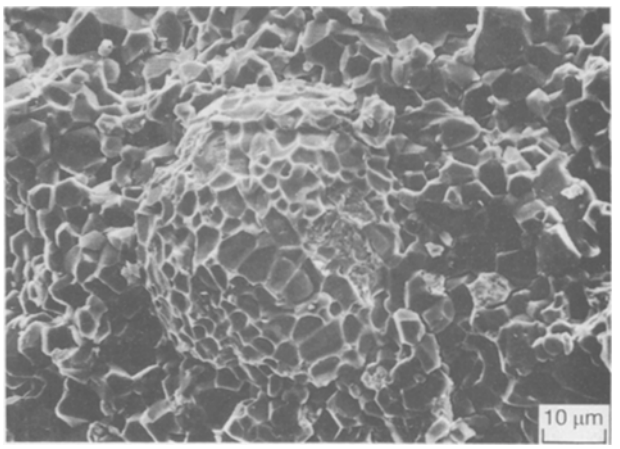

Figure 7 SEM photograph showing the fracture surface of a composite containing 10 vol % TZ-12Ce agglomerates without chemical etching.

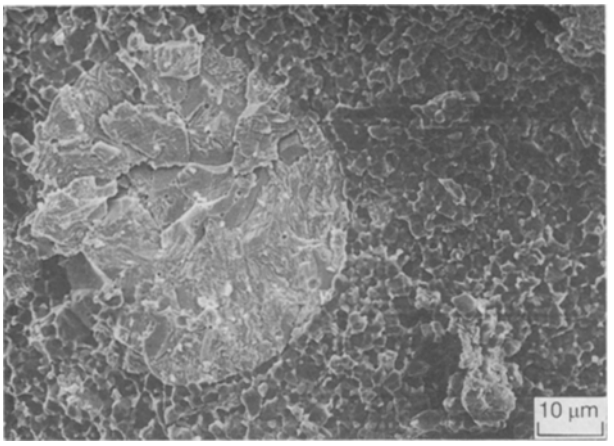

Figure 8 SEM photograph showing the fracture surface of a composite containing 10 vol % TZ-12Ce agglomerate with chemical etching.

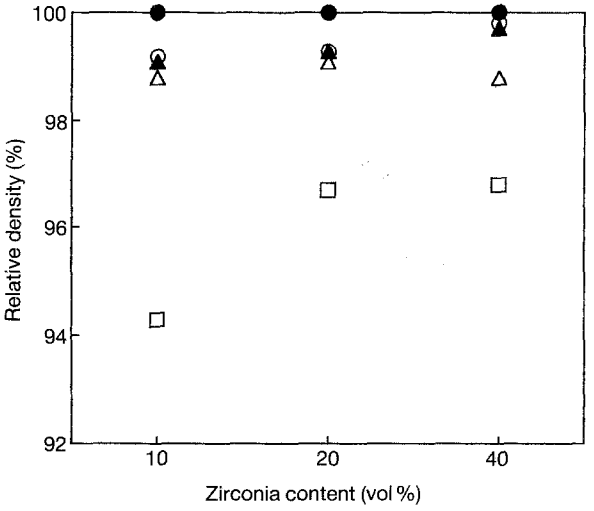

Figure 9 Relationship between the relative density of composites with 10 vol % agglomerate and the volume fraction of zirconia particles before and after post-HIPing (A) Al_2O_3, (O) TZO, (Y) TZ-3Y, (Ce) TZ-12Ce, (KY) TZ-3Y agglomerate, (KCe) TZ-12Ce agglomerate, (KO) TZO agglomerate, (number is the volume fraction). □, A:Ce:KY; ○, A:Y:KCe; △, A:Y:KO, ▲, A:Y:KO (HIP–1500, 100); ●, A:Y:KCe (HIP–1600, 150).

1600 °C for 10 h in air) were 99% for Al_2O_3–TZO, 99.7% for Al_2O_3–TZ-3Y and 100% for Al_2O_3–TZ-12Ce, respectively. As pointed out in [1], the densification of the multiphase composite was significantly governed by the shape and size of the zirconia particle. Also, grain growth of the alumina particle was eventually controlled by dispersion of the zirconia particle. Table I lists the relative densities of composites with two kinds of zirconia agglomerate dispersed (10 vol % each) into the alumina matrix, sintered at 1600 °C for 10 h in air. It was realized that the low densification of the composite was attributed to the large size of the agglomerate. As seen in this table, chemical etching on the surface of the agglomerates had, however, the advantage of densification of the composites with dispersed agglomerates into the alumina matrix. Furthermore, the relative densities of the composites could be elevated by further adding the fine particle of zirconia as shown in Table II.

Fig. 9 shows the relationship between the relative density of the composite with dispersed 10 vol % zirconia agglomerates and the content of the zirconia particle before and after post-HIPing. It was found that the addition of zirconia particles effected the densification of composites fabricated by a conventional sintering method. However, the lowering of the relative densities for the composite containing TZ-3Y agglomerates was reasonably caused by the formation of macrocracks, as shown in Fig. 5. After HIPing, the relative densities of composites were significantly increased, and reached the theoretical value. When TZ-12Ce and TZO agglomerates with chemical etching were used, the composites with a duplex structure were well densified by conventional sintering techniques, and the post-HIP sintering procedure was further available for densification of the composites.

Fig. 10 shows the crack propagation profile introduced by Vickers indentation. As seen in this photograph, a crack started from the apex of the diamond indentor, was deflected and stopped within the zirconia agglomerate. The thermal expansion coefficient

TABLE I Relative densities of composites dispersed with two kinds of zirconia agglomerate into the alumina matrix

Sample (vol %)	A:KO:KCe[a] (80:10:10)	A:KCe:KY[a] (80:10:10)
Without chemical etching	77.8%	83.1%
With chemical etching	93.8%	94.4%

[a] (A) Al_2O_3, (KO) TZO agglomerate, (KCe) TZ-12Ce agglomerate, (KY) TZ-3Y agglomerate.

TABLE II Relative densities of multiphase composites with dispersed zirconia agglomerate into alumina–zirconia matrices

Sample (vol %)	A:KY:O[a] (80:10:10)	A:KY:Ce[a] (80:10:10)	A:KO:Y[a] (80:10:10)	A:KCe:Y[a] (80:10:10)
Sintered at 1600 °C in air	96.7%	94.5%	98.3%	98.7%
Post-HIPing	98.5%	–	98.5%	100.0%

[a] (O) TZO, (Ce) TZ-12Ce, (Y) TZ-3Y, (A) Al_2O_3, (KO) TZO agglomerate, (KCe) TZ-12Ce agglomerate, (KY) TZ-3Y agglomerate.

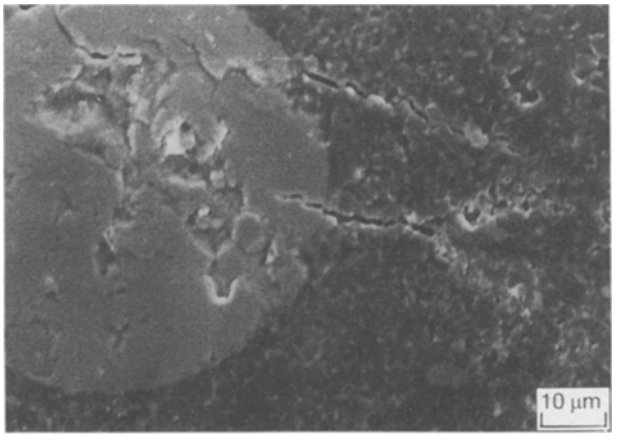

Figure 10 SEM photograph of serious crack propagation introduced by Vickers indentation.

of zirconia is larger than that of Al_2O_3 [9]. It was, consequently, plausible that greater shrinkage of the agglomerate was attained on cooling to room temperature. As a result, it was considered that the supplementary tension of the interior of the agglomerate had the privilege of absorbing the stress energy of the crack propagation.

Fig. 11 shows the bending strength of various composites. Even though the content of zirconia was the same throughout, the bending strength of composites containing agglomerates tended to decrease. Fig. 12 shows the bending strength of composites before and after post-HIPing as a function of zirconia particle content. In the composites dispersed with TZO agglomerates, the effect of post-HIPing on improvement of the bending strength was scarcely observed. On the other hand, the bending strength of composites with dispersed TZ-12Ce agglomerates remarkably increased up to 760 MPa after HIPing. The discrepant

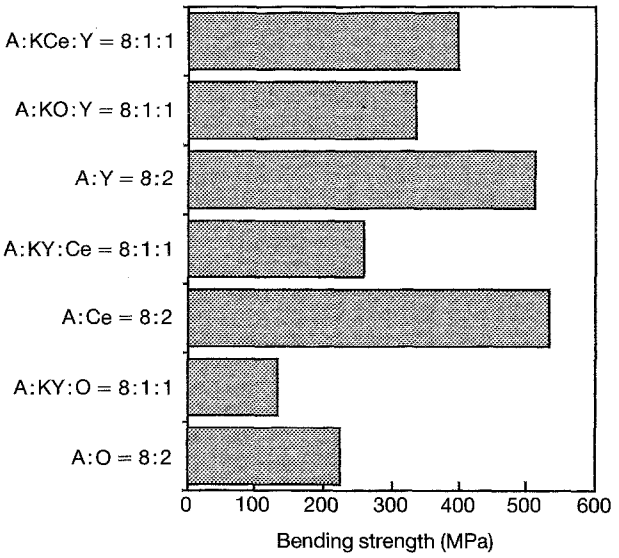

Figure 11 Bending strength of composites (notation is the same as shown in Fig. 9).

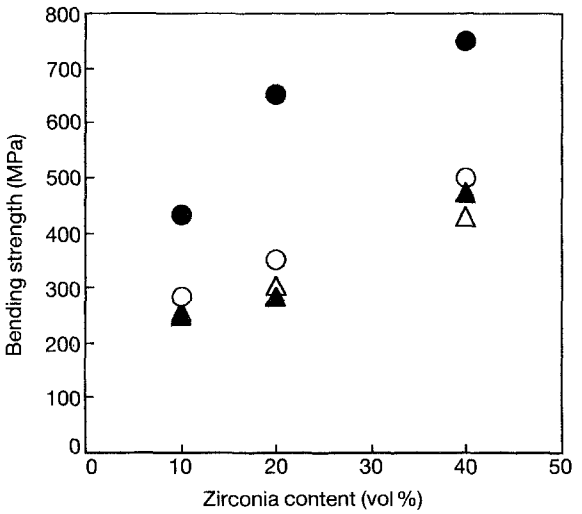

Figure 12 Relationship between the bending strength of composites with 10 vol % agglomerate and the volume fraction of the zirconia particle before and after post-HIPing (notation is the same as in Fig. 9). △, A:Y:KO; ○, A:Y:KCe; ●, A:Y:KCe (HIP); ▲ A:Y:KO (HIP).

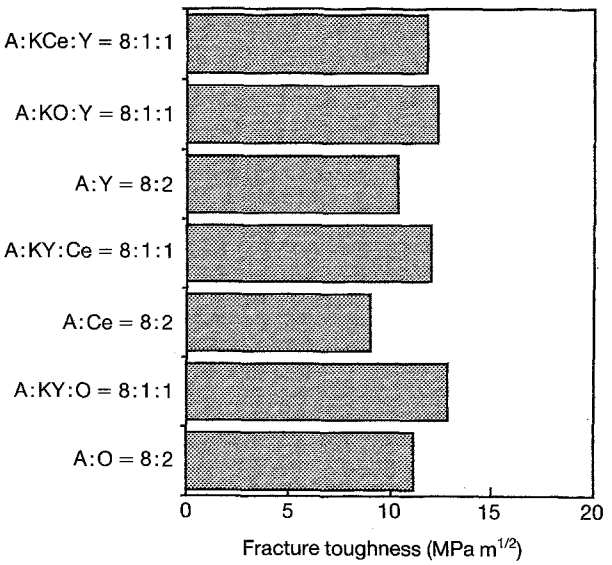

Figure 13 Fracture toughness of composites (notation is the same as shown in Fig. 9).

profile was entirely due to the shape of the agglomerate. This is the main reason why the energy of crack propagation was little consumed by inhomogeneity of the bending strain generated around granular TZO agglomerates [10]. In addition, it was concluded that the dispersion of spherical TZ-12Ce agglomerates was effective and available for controlling mechanical properties.

Fig. 13 shows the fracture toughness of the composites determined by an indentation fracture method. As seen in this figure, all multiphase composites of dispersed zirconia agglomerate demonstrate relatively higher values of fracture toughness, e.g. values in excess of $K_{1c} = 11$ MPa m$^{1/2}$ which are measured for composites dispersed with 20 vol % TZO particles into the alumina matrix (denoted as A : O = 8 : 2 in this figure).

4. Conclusions

In summary, it was found that the nature of interfacial bonding of the zirconia agglomerate with the alumina matrix was drastically improved by acidic etching. In addition, the difference in thermal expansion characteristics between the agglomerate and the matrix may enhance the mechanical stress, especially tension, which prefers to confine the movement of the crack towards the agglomerates, thereby increasing fracture toughness.

Also, it was of great advantage to deflect the crack propagation in and out of the agglomerates, which were composed of spherical agglomerates with a few microns of tetragonal zirconia polycrystallines.

Acknowledgements

This work was supported, in part, by a Grant-in-Aid for Developmental Scientific Research (B) of the Ministry of Education, Science and Culture.

References

1. N. CLAUSSEN, J. STEEB and R. PABST, *Amer. Ceram. Soc. Bull.* **55** (1977) 559.
2. N. CLAUSSEN and E. LUTZ, in "Proceedings of the International Symposium on Fine Ceramics" Arita, Vol. **2** (Saga Pref, Japan 1987) p. 3.
3. J. WANG and R. STEVENS, *J. Mater. Sci.* **24** (1989) 3421.
4. K. TUKUMA and K. UEDA, *J. Amer. Ceram. Soc.* **68** (1985) C-4–C-5.
5. R. STEVENS and P. A. EVANS, *Br. Ceram. Trans. J.* **83** (1984) 28.
6. J. WANG and R. STEVENS, *J. Mater. Sci.* **23** (1988) 804.
7. K. NIIHARA, R. MORENA and D. P. H. HASSELMAN, *ibid.* **1** (1982) 13.
8. D. P. H. HASSELMAN, *J. Amer. Ceram. Soc.* **53** (1970) 490.
9. F. A. HUMMEL, *ibid.* **33** (1950) 103.
10. O. SUDRE, G. BAO, B. FAN, F. F. LARGE and A. G. EVANS, *ibid.* **75** (1992) 525.

Received 28 January
and accepted 8 October 1993